

AD-A079 308

ELECTROMECHANICAL SYSTEMS OF NEW MEXICO INC ALBUQUERQUE F/G 8/13  
DYNAMIC STRESS-STRAIN MEASUREMENTS ON MISERS BLUFF.(U)

MAY 79 R A SHUNK

DNA001-78-C-0260

UNCLASSIFIED

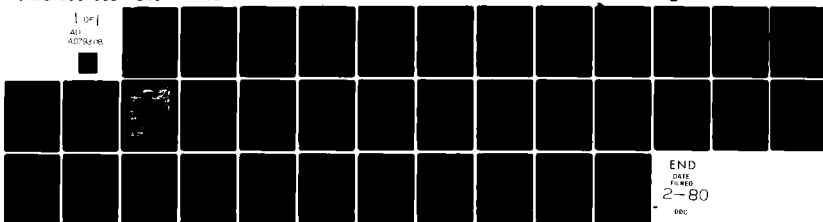
ESI-79-002-TR

DNA-4970T

NL

1 of 1

ALL  
ADDITIONAL



END

DATE

FILED  
2-80

DDC

AD-E300 637

(12)

DNA 4970T

# DYNAMIC STRESS-STRAIN MEASUREMENTS ON MISERS BLUFF

Electromechanical Systems of New Mexico, Inc.  
P.O. Box 11730  
Albuquerque, New Mexico 87192

1 May 1979

Topical Report for Period 1 May 1978—30 April 1979

CONTRACT No. DNA 001-78-C-0260

APPROVED FOR PUBLIC RELEASE;  
DISTRIBUTION UNLIMITED.

THIS WORK SPONSORED BY THE DEFENSE NUCLEAR AGENCY  
UNDER RDT&E RMSS CODE B344079462 J11AAXSX35257 H2590D.

Prepared for  
Director  
DEFENSE NUCLEAR AGENCY  
Washington, D. C. 20305

22 5 040

ADA 079308

DDC FILE COPY

Destroy this report when it is no longer  
needed. Do not return to sender.

PLEASE NOTIFY THE DEFENSE NUCLEAR AGENCY,  
ATTN: STTI, WASHINGTON, D.C. 20305, IF  
YOUR ADDRESS IS INCORRECT, IF YOU WISH TO  
BE DELETED FROM THE DISTRIBUTION LIST, OR  
IF THE ADDRESSEE IS NO LONGER EMPLOYED BY  
YOUR ORGANIZATION.



UNCLASSIFIED

SECURITY CLASSIFICATION OF THIS PAGE (When Data Entered)

REPORT DOCUMENTATION PAGE		READ INSTRUCTIONS BEFORE COMPLETING FORM
1. REPORT NUMBER DNA 4970T, AD E2 11-30	2. GOVT ACCESSION NO.	3. RECIPIENT'S CATALOG NUMBER
4. TITLE (and Subtitle) DYNAMIC STRESS-STRAIN MEASUREMENTS ON MISERS BLUFF,	5. TYPE OF REPORT & PERIOD COVERED Topical Report, for Period 1 May 78-30 Apr 1979	6. PERFORMING ORG. REPORT NUMBER ESI-79-002-TR
7. AUTHOR(s) R. A. Shunk	8. CONTRACT OR GRANT NUMBER(s) DNA 001-78-C-0260	9. PROGRAM ELEMENT, PROJECT, TASK AREA & WORK UNIT NUMBERS Subtask J11AAXSX352-57
10. PERFORMING ORGANIZATION NAME AND ADDRESS Electromechanical Systems of New Mexico, Inc. P.O. Box 11730 Albuquerque, New Mexico 87192	11. CONTROLLING OFFICE NAME AND ADDRESS Director Defense Nuclear Agency Washington, D.C. 20305	12. REPORT DATE 1 May 1979
13. MONITORING AGENCY NAME & ADDRESS (if different from Controlling Office) DNA	14. NUMBER OF PAGES 36	15. SECURITY CLASS (of this report) UNCLASSIFIED
15a. DECLASSIFICATION/DOWNGRADING SCHEDULE		
16. DISTRIBUTION STATEMENT (of this Report)  Approved for public release; distribution unlimited.		
17. DISTRIBUTION STATEMENT (of the abstract entered in Block 20, if different from Report)		
18. SUPPLEMENTARY NOTES  This work sponsored by the Defense Nuclear Agency under RDT&E RMSS Code B344079462 J11AAXSX35257 H2590D.		
19. KEY WORDS (Continue on reverse side if necessary and identify by block number) Soil Strain Dynamic Soil Strain Strain Gage High Explosives MISERS BLUFF, Phase II		
20. ABSTRACT (Continue on reverse side if necessary and identify by block number) MISERS BLUFF, Phase II, Test 2 was the near simulation explosion of six 120 ton ANFO charges on the corner of a hexagon 100 m on a side. Soil stress and strain measurements at several depths were made 6 m from the array center and between two charges. During the compressive loading by the air blast, dynamic stress-strain curves were plotted where data are available. Comparing the two locations shows different material behavior. Also, the near surface stress gages did not reproduce the air shock structure indicating a peculiarity of the		

DD FORM 1 JAN 73 1473 EDITION OF 1 NOV 65 IS OBSOLETE

UNCLASSIFIED

SECURITY CLASSIFICATION OF THIS PAGE (When Data Entered)

212

UNCLASSIFIED

SECURITY CLASSIFICATION OF THIS PAGE(When Data Entered)

20. ABSTRACT (Continued)

material or material-gage interaction process. The material in the test bed exhibited a large strain energy absorption for propagating stress waves.

X

UNCLASSIFIED

SECURITY CLASSIFICATION OF THIS PAGE(When Data Entered)

## PREFACE

The measurements of stress and strain on MISERS BLUFF, Phase II that are discussed here were made by the Waterways Experiment Station under the direction of personnel from the Weapons Effects Laboratory. Mr. Don Day and Mr. Don Murrell have been most helpful in obtaining data and in supervising the installation of the gages in the field. Mr. John Stout did the gage placement which turned out to be more difficult than anticipated because of the lack of a cohesive soil. Operation of the recording facility was done by Mr. Jim Pickens. My thanks to these people and others at WES who were responsible for the successful execution of this part of the experiment. The DNA Test Group Director was LCDR J. D. Strode and the Technical Director was Capt. Robert DeRaad. This work was done under contract to DNA on Contract DNA001-78-C-0260.

[illegible]

## TABLE OF CONTENTS

<u>Section</u>		<u>Page</u>
I	INTRODUCTION	5
II	DYNAMIC STRESS-STRAIN MEASUREMENTS	7
III	CONCLUSIONS AND RECOMMENDATIONS	10

## LIST OF ILLUSTRATIONS

<u>Figure</u>		
1	Measurement and charge locations for the stress-strain measurements on Misers Bluff-Phase II. Horizontal stresses are measured in the directions of the arrows at the measurement locations.	6
2	Surface overpressure near the stress-strain measurement locations at 87 m, 240° azimuth.	11
3	Diaphragm stress gages partially uncovered for measuring vertical and horizontal stress.	12
4	Vertical stress at 87 m, 0.3 m depth and 240° azimuth.	13
5	Horizontal stress at 87 m, 0.3 m depth and 240° azimuth.	14
6	Vertical strain at 87 m, 0.3 m depth and 240° azimuth.	15
7	Horizontal stress at 87 m, 0.6 m depth and 240° azimuth	16
8	Vertical strain at 87 m, 0.6 m depth and 240° azimuth.	17
9	Vertical stress at 87 m, 1.2 m depth and 240° azimuth.	18

# LIST OF ILLUSTRATIONS (Continued)

<u>Figure</u>		<u>Page</u>
10	Horizontal stress at 87 m, 1.2 m depth and 240 <sup>0</sup> azimuth.	19
11	Vertical strain at 87 m, 1.2 m depth and 240 <sup>0</sup> azimuth.	20
12	Dynamic stress-strain curves for three depths at 87 m, 240 <sup>0</sup> azimuth.	21
13	Air blast wave form at 180 <sup>0</sup> and 6 m from center of the array over strain gage emplacement.	22
14	Vertical stress at 6 m, 0.3 m depth and 180 <sup>0</sup> azimuth.	23
15	Horizontal stress at 6 m, 0.3 m depth and 180 <sup>0</sup> azimuth.	24
16	Horizontal stress at 6 m, 0.6 m depth and 180 <sup>0</sup> azimuth.	25
17	Vertical strain from 6 m, 0.6 m depth and 180 <sup>0</sup> azimuth.	26
18	Horizontal stress from 6 m, 0.9 m depth and 180 <sup>0</sup> azimuth.	27
19	Vertical strain from 6 m, 0.9 m depth and 180 <sup>0</sup> azimuth.	28
20	Vertical stress from 6 m, 1.2 m depth and 180 <sup>0</sup> azimuth.	29
21	Horizontal stress at 6 m, 1.2 m depth and 180 <sup>0</sup> azimuth.	30
22	Vertical strain at 6 m, 1.2 m depth and 180 <sup>0</sup> azimuth.	31
23	Dynamic stress-strain curves for three depths at 6 m, 180 <sup>0</sup> azimuth.	32



## SECTION I

### INTRODUCTION

MISERS BLUFF, Phase II, Test 2 was the near simultaneous explosion of six 120 ton ANFO charges on the corners of a hexagon 100 m on a side. The details of the experiment are described in Reference 1.

There were stress and strain measurements made at three places in the test bed and at several depths shown in Figure 1 (Reference 2). The comparison of stress and strain at the same time at the same depth will produce a dynamic stress-strain curve of the material reaction. The resulting curve may be markedly different from a static uniaxial stress-strain curve and can only be checked against a dynamic calculation. The air shock wave speeds are very high compared to the material wave velocity and the waves are relatively long compared to gage depths, so the initial compressive motion should be uniaxial, but after a time, effects from other parts of the test bed will be seen. Reflections from layers, waves from cratering regions and high shock pressure regions that develop through shock-shock interactions will all perturb the test bed in a three dimensional way. Therefore, only the compressive phase of the data is being considered.

Analysis of the dynamic stress-strain data shows different behavior in two different parts of the test bed, although large energy absorption in the soil is indicated. The air shock structure is not reproduced in the stress records from shallow gages and significant attenuation of the peak pressure is observed with depth.

- 
1. "Misers Bluff Series; Phase II, Ground Shock and Airblast Measurements Data Report", Final Report, WES, M.P.N.-78-4, June 1978.
  2. "Soil Strain Measurements on Misers Bluff - Phase II", DNA Topical Report, R. A. Shunk (unpublished).

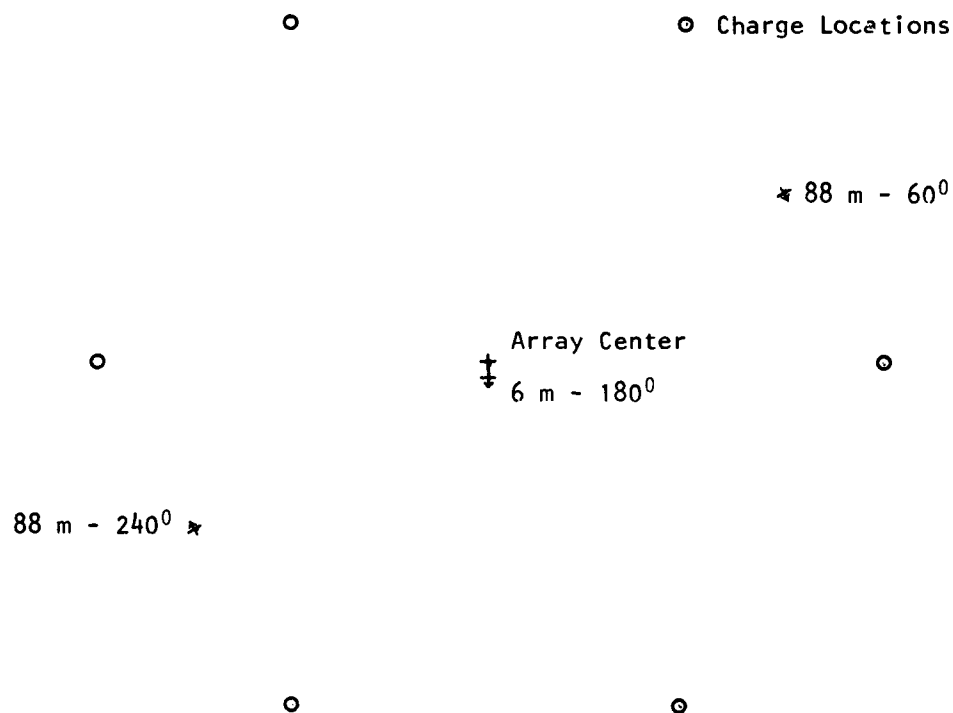


Figure 1. Measurement and charge locations for the stress-strain measurements on Misers Bluff-Phase II. Horizontal stresses are measured in the directions of the arrows at the measurement locations.

## SECTION II

### DYNAMIC STRESS-STRAIN MEASUREMENTS

The strain measurements were made with a telescoping spool gage (Reference 2) with a span of 2 cm. The output was derived from a linear variable differential transformer with a linear range of 5 cm. The stress measurements were made with the Waterways Experiment Station (WES) "SE" gage, a small diaphragm-type stress gage (Reference 3). The diaphragm deflection is detected by strain gages cemented to the diaphragm. All signals were recorded on magnetic tape as analogue voltages which were later digitized and plotted at WES.

The material in the upper meter of the test bed where these measurements were made was a weak aeolian soil with a void ratio of 40% (Reference 4).

Unfortunately, the return from the stress data was not as high as desired and some gages did not produce data for one reason or another. Thus, at several depths, only horizontal stress data are available. The data at 1.2 m depth and at 0.3 m depth at the 6 m - 180 station shows that the vertical stress is twice the horizontal stress. So to get the dynamic stress-strain curves in Figure 12, the horizontal stress was multiplied by two to get an estimate of the vertical stress. The supporting stress and strain records for 240 - 87.7 m are shown in Figures 7 through 11.

The curves in Figure 12 show the strain decreasing with depth. The peak strain is -17%, well within the gage range of -22% (negative strain

- 
3. Ingram, T. D., "Development of a Free-Field Soil Stress Gage for Static and Dynamic Measurements," Technical Report No. 1-814, Feb. 1968, U.S. Army Engineer Waterways Experiment Station, CE, Vicksburg, Miss.
  4. Jackson, Ed, "Geotechnical Investigation for Misers Bluff II" in the Misers Bluff Phase II Symposium Report, POR 7013, (unpublished), U.S. Army Engineer Waterways Experiment Station, Vicksburg, Miss.

is compressive). The peak stress is not falling off with depth. An increase in stress at 1.2 m over the stress at 0.6 m cannot be explained. The large open loop of the stress-strain curves indicates large energy absorption.

The data from the area at 6 m range, 180° from the array center will be examined next. The overpressure waveform is shown in Figure 13. The data from the two stress gages at 0.3 m are shown in Figures 14 and 15. A large attenuation in pressure is apparent. The strain record at 0.3 m is not credible because the form indicates gage failure and will not be discussed. The main point of showing these near surface gage records is to point out how the structure in the air pressure appears to be washed out by the soil or the combination of soil and stress gage interaction. A similar thing happened at 240° but one of the lower gages (Figure 7) seems to show the air pressure structure.

The response of the shallow stress gages to the multiple spikes in the air pressure waves is indicative of material response after the initial air shock loading that is not understood. For example, the air shock wave histories at both locations contain several spikes. At 87 m, 240° there are two very distinct spikes of about the same amplitude (Figure 2). The stress gage records at 0.3 m depth, Figure 4 and 5, show no indication of the second spike. There is a problem here in that the horizontal stress recorded is higher than the overpressure which is unlikely. The horizontal stress gages were oriented with the sensitive direction toward the nearest charge. A sharp third spike of about two thirds the amplitude of the first two appears in the pressure wave at about 23 msec. There is a rise in the vertical stress record at the correct time to represent this air pressure spike but it only goes to about 0.40 of the peak stress value. At 6 m - 180°, there is a somewhat similar effect where the first vertical stress rise in Figure 14 is about the same as the air pressure rise in Figure 13, about 2 Mpa. The air pressure wave decays slightly and two more distinct spikes follow in the air pressure record. These are reproduced in time in the stress record but very poorly in amplitude. The stress gage shows 3.1 Mpa compared to 9 Mpa for the third air shock. The horizontal stress gage in Figure 15 shows sharper rise times but lower amplitudes and in

both instances the second spike is lower than the first. Soil strain at 87 m,  $240^{\circ}$  is less than -10% when the second spike arrives. Soil strain at 6 m,  $180^{\circ}$  is probably on the order of -10% when the second spike arrives. Thus, some change occurs in the material and/or the stress gage which, after the material is compacted and partially unloaded in stress but not in strain, does not allow the stress gage to respond to the surface pressure less than 0.3 m away.

The initial soil stresses and accelerations are quite high near the surface and one can conjecture about differential motion between the outer protective steel ring of the stress gage and the less dense gage body. The ring is there to remove the cross axis sensitivity of the gage. (A soft rubbery material separates the two.) If this motion were significant, the stress gage body would be exposed to edge effects created by the ring that is supposed to protect it, causing a distorted waveform. Theoretically, this would only occur during the initial wavefront passage, but could have a lasting effect on gage response.

The dynamic stress-strain data for  $180^{\circ}$  - 6 m are shown in Figure 23 for three depths where stress measurements are available. They show an open loop response but have a stress cutoff unlike the data at  $240^{\circ}$ . There is a definite decrease in peak compressive strain with depth. The supporting data are shown in Figures 16 through 22.

### SECTION III

#### CONCLUSIONS AND RECOMMENDATIONS

How much the different material reactions in the two measurement locations depend on the peak overpressure, overpressure waveforms and the interactive material properties cannot be sorted out by inspecting these data. However, it is clear that a large amount of energy is dissipated in this material during shock loading. The stress gage and material response to multiple shock loadings needs to be explained if the stress data are to have much value.

Modeling of the material and some high pressure, one dimensional shock loading tests of similar materials in a realistically scaled facility could be used to get some additional information on dynamic stress-strain behavior. A one dimensional experiment would be valuable where stress, strain and acceleration-velocity can be measured with multiple step surface loads of on the order of 2 to 10 Mpa. A one dimensional calculational effort using a material model structured around the MISERS BLUFF soil might give the clues necessary to explain the stress data obtained on MISERS BLUFF, Phase II, Test 2.

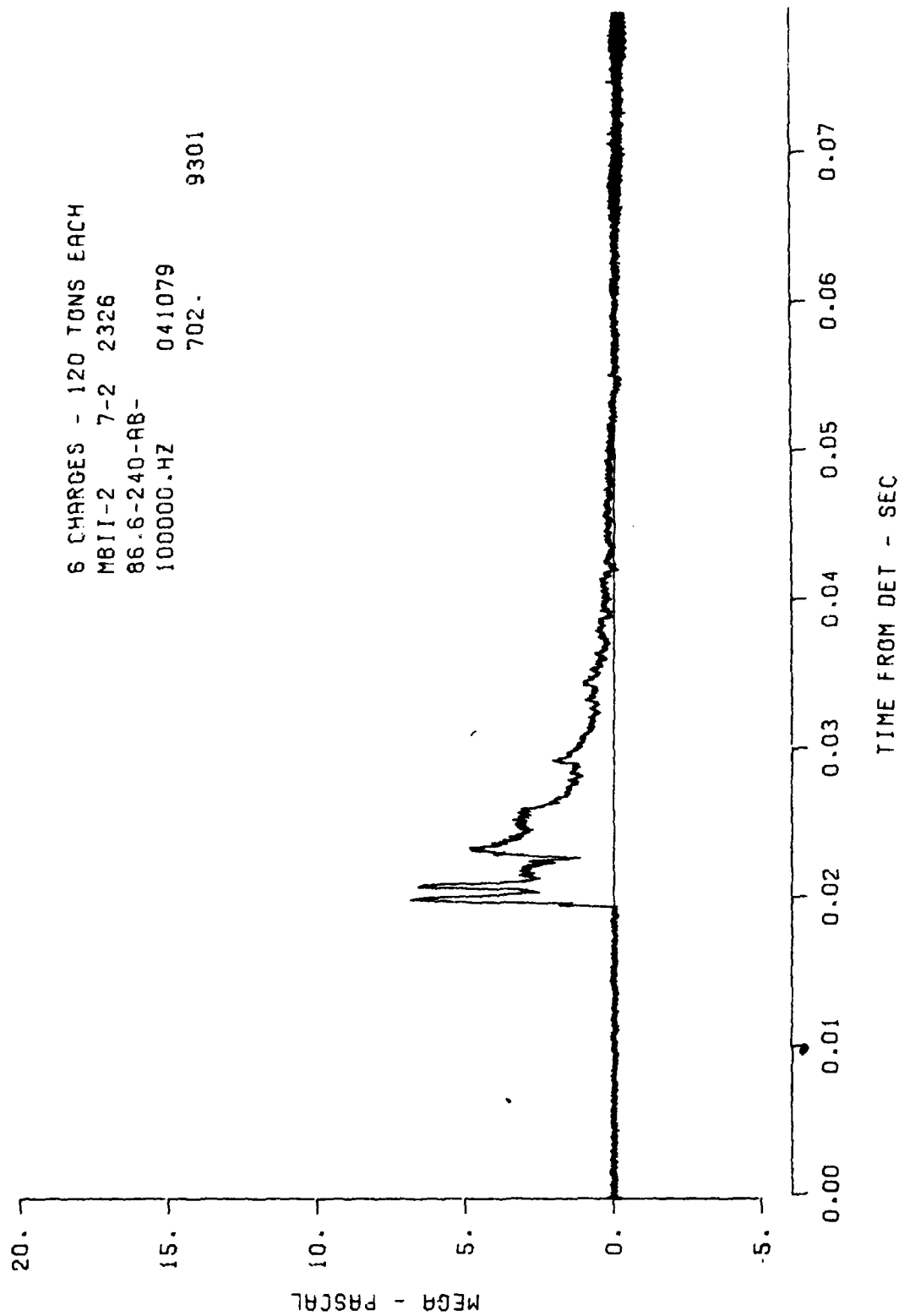


Figure 2. Surface overpressure near the stress-strain measurement locations at 87 m, 240° azimuth.



Figure 3. Diaphragm stress gages partially uncovered for measuring vertical and horizontal stress.



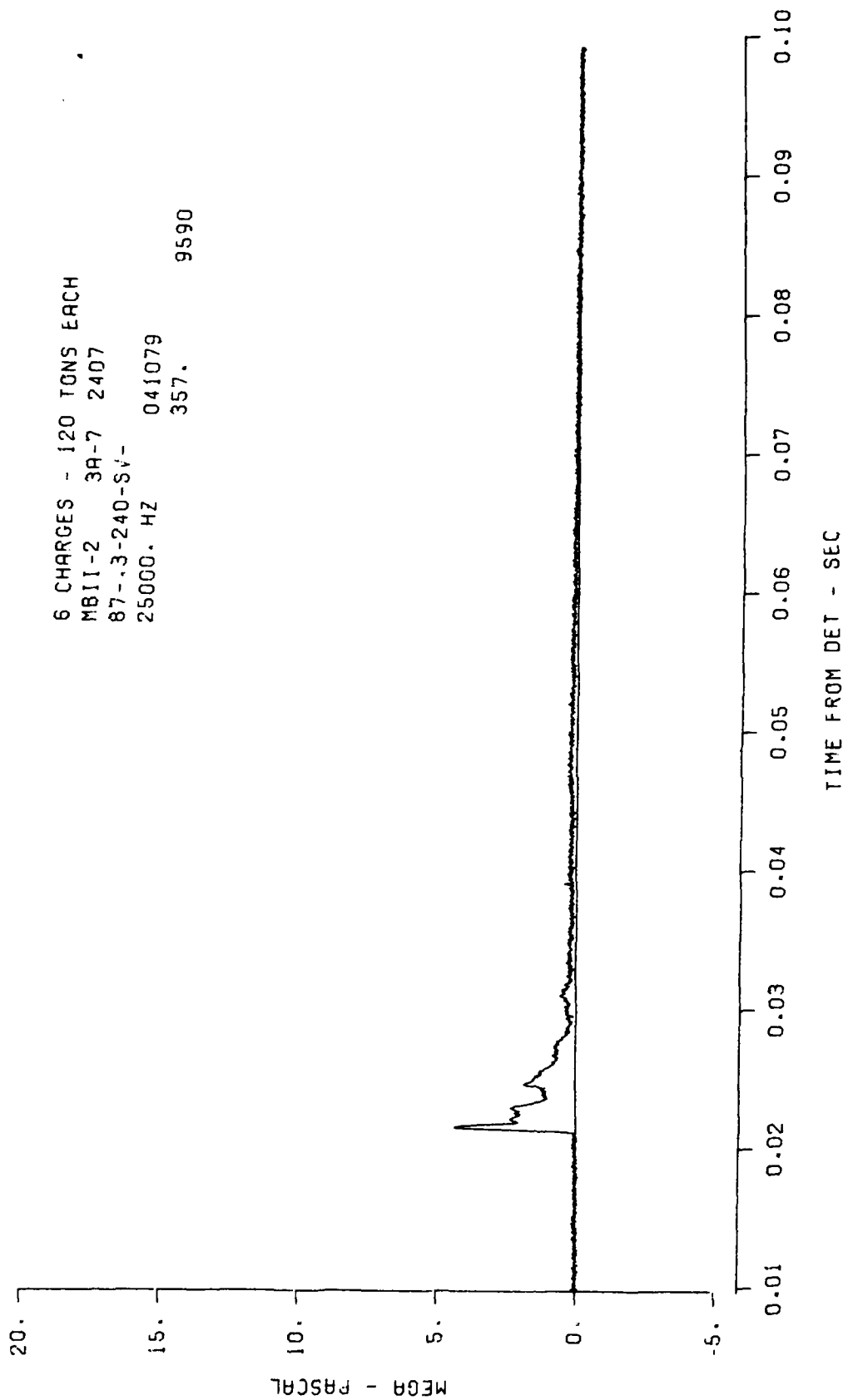


Figure 4. Vertical stress at 87 m, 0.3 m depth and 240° azimuth.

6 CHARGES - 120 TONS EACH  
 MBII-2 3A-8 2408  
 87-.3-240-SH-240  
 25000. HZ 041079 9590  
 358.

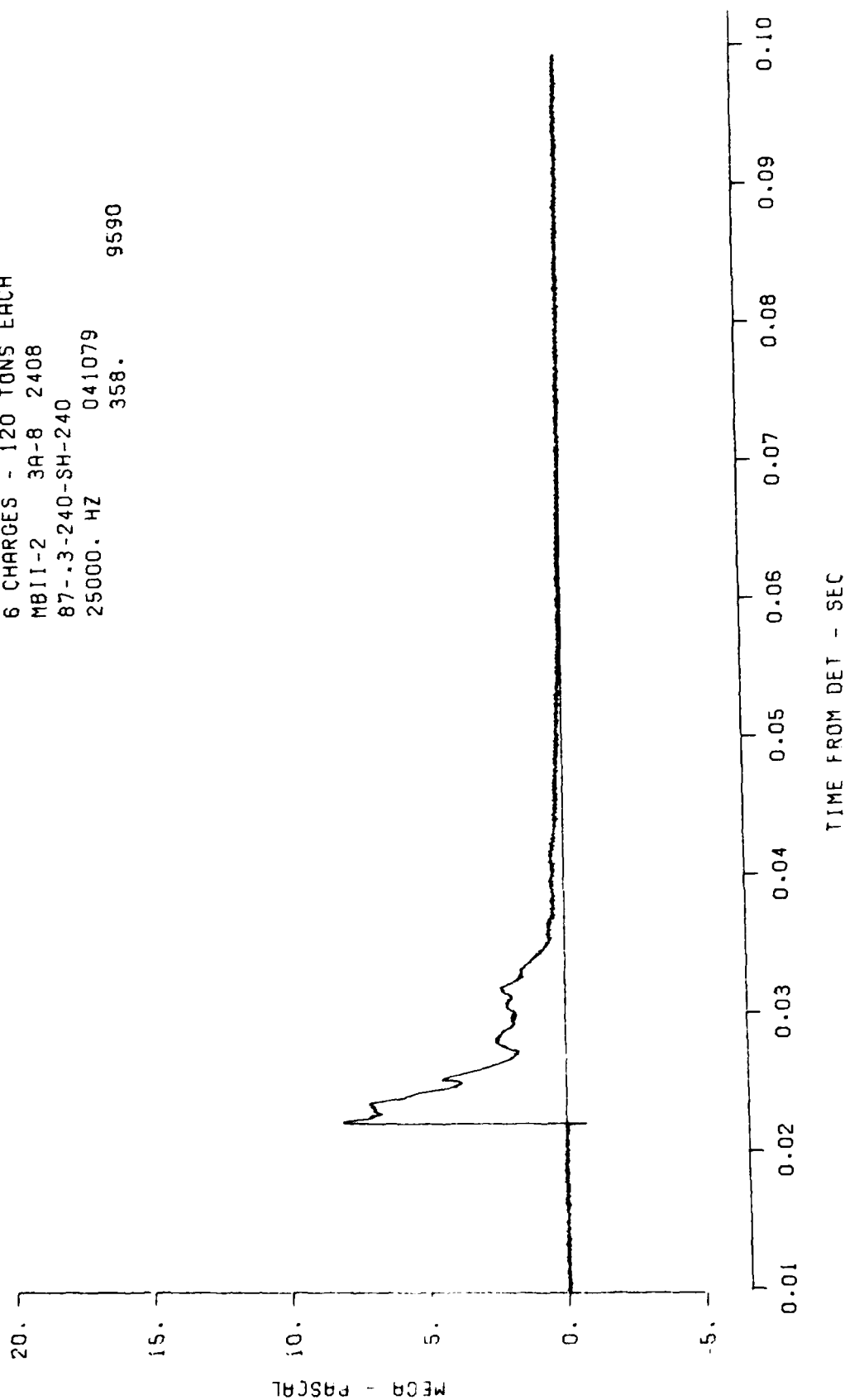


Figure 5. Horizontal stress at 87 m, 0.3 m depth and 240° azimuth.

6 CHARGES - 120 TONS EACH  
MBII-2 6-7 2612  
87-.3-240-0-12-  
25000. HZ 041079 9790  
107.

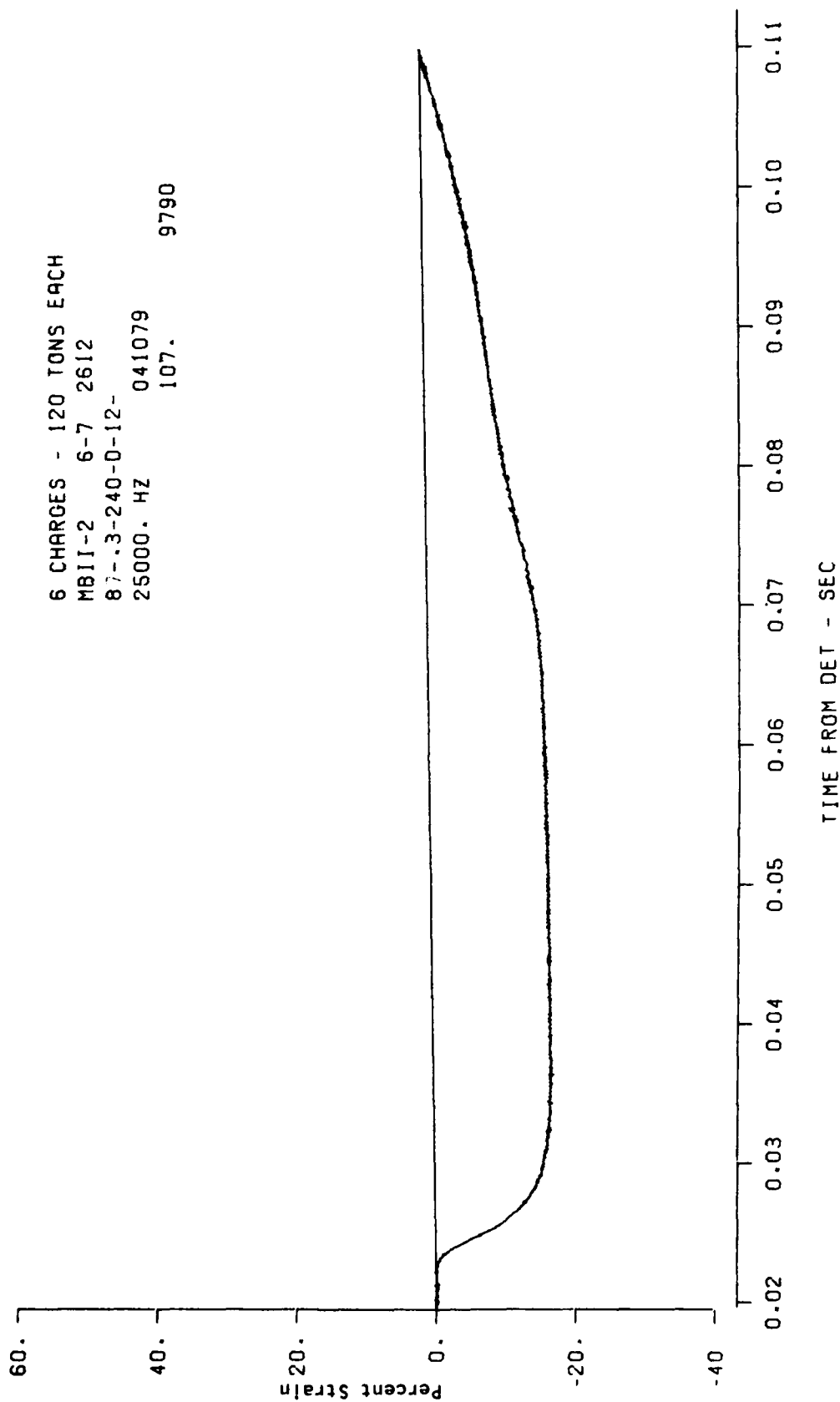


Figure 6. Vertical strain at 87 m, 0.3 m depth and 240° azimuth.

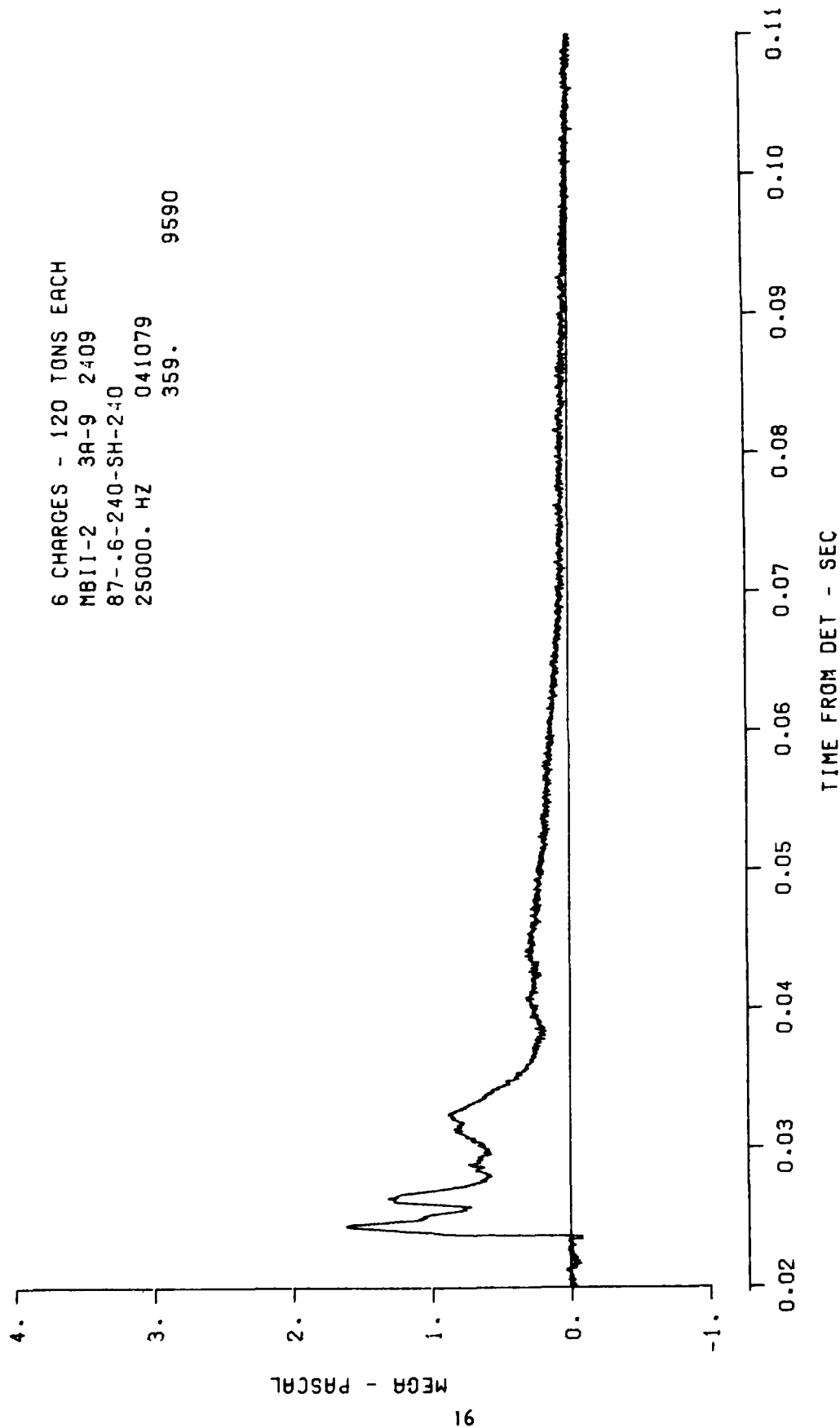


Figure 7. Horizontal stress at 87 m, 0.6 m depth and 240° azimuth.

6 CHARGES - 120 TONS EACH  
 MB11-2 6-9 2614  
 87-.6-240-D-14-  
 25000. HZ 041079 9790  
 109.

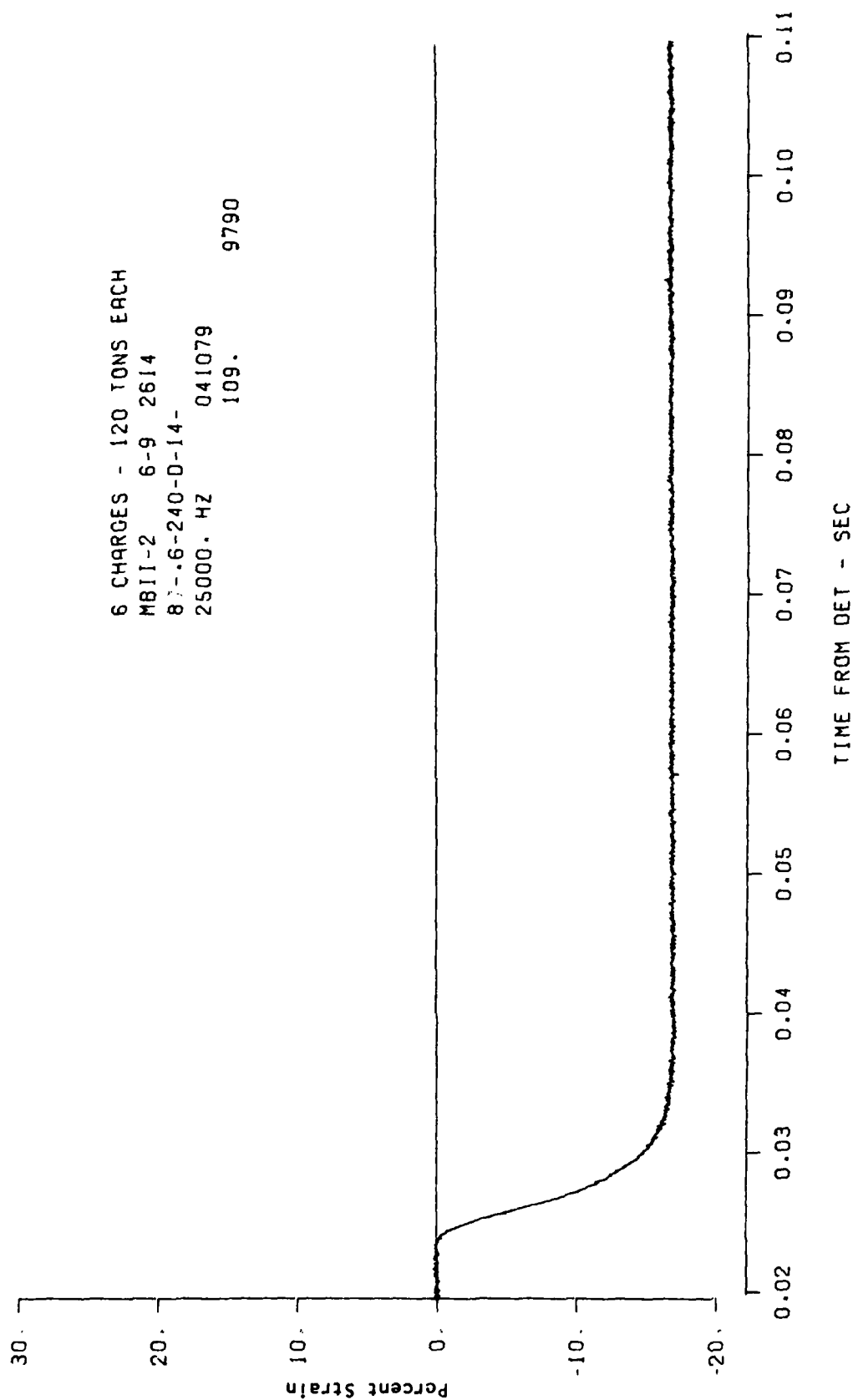


Figure 8. Vertical strain at 87 m, 0.6 m depth and 240° azimuth.

6 CHARGES - 120 TONS EACH  
MBII-2 3A-11 2411  
87-1.2-240-SV-  
25000. HZ 041079  
361. 9590

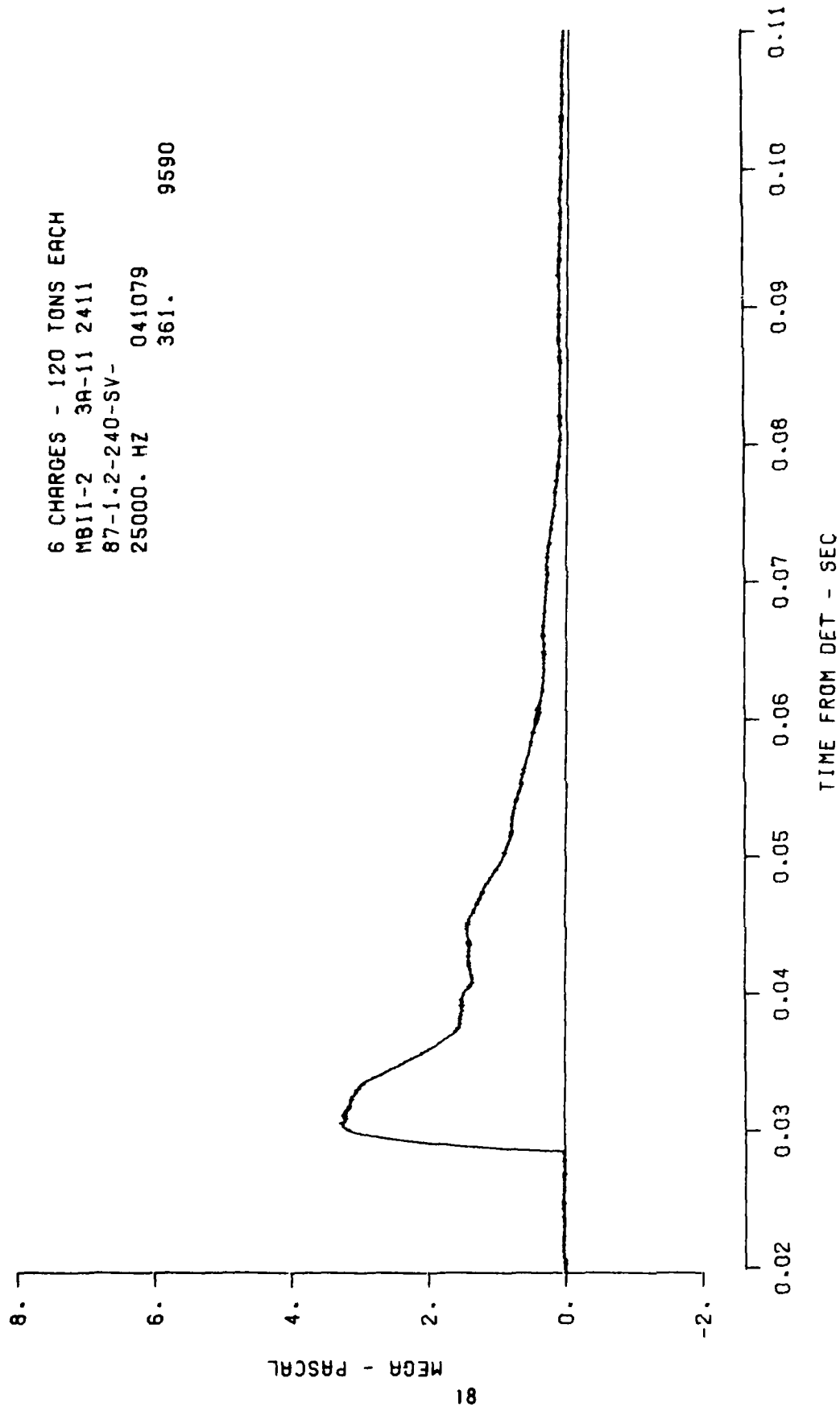


Figure 9. Vertical stress at 87 m, 1.2 m depth and 240° azimuth.

6 CHARGES - 120 TONS EACH  
MBII-2 3A-12 24i2  
87-1.2-240-SH-240  
25000. HZ 041079 9590  
362.

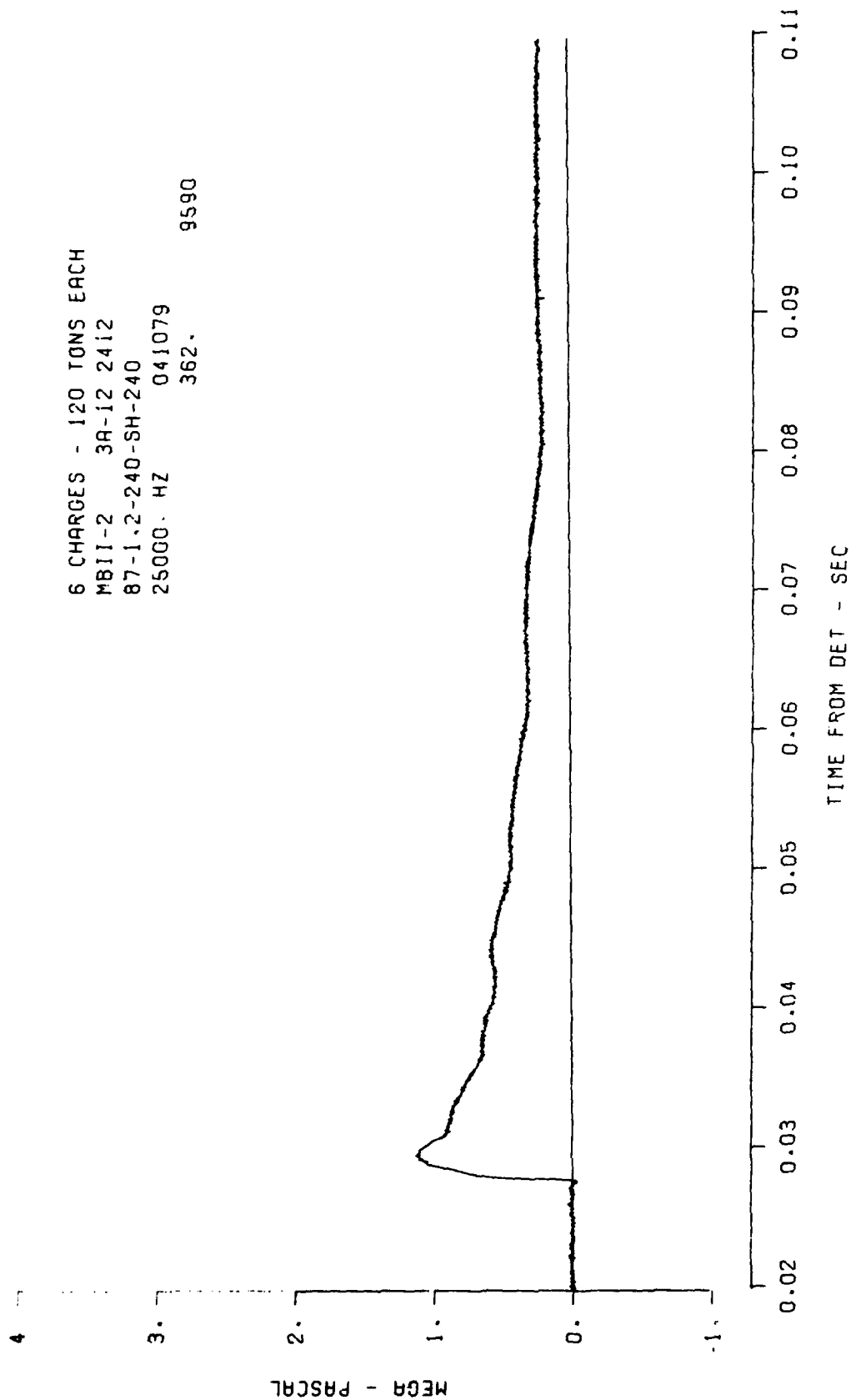


Figure 10. Horizontal stress at 87 m, 1.2 m depth and 240° azimuth.

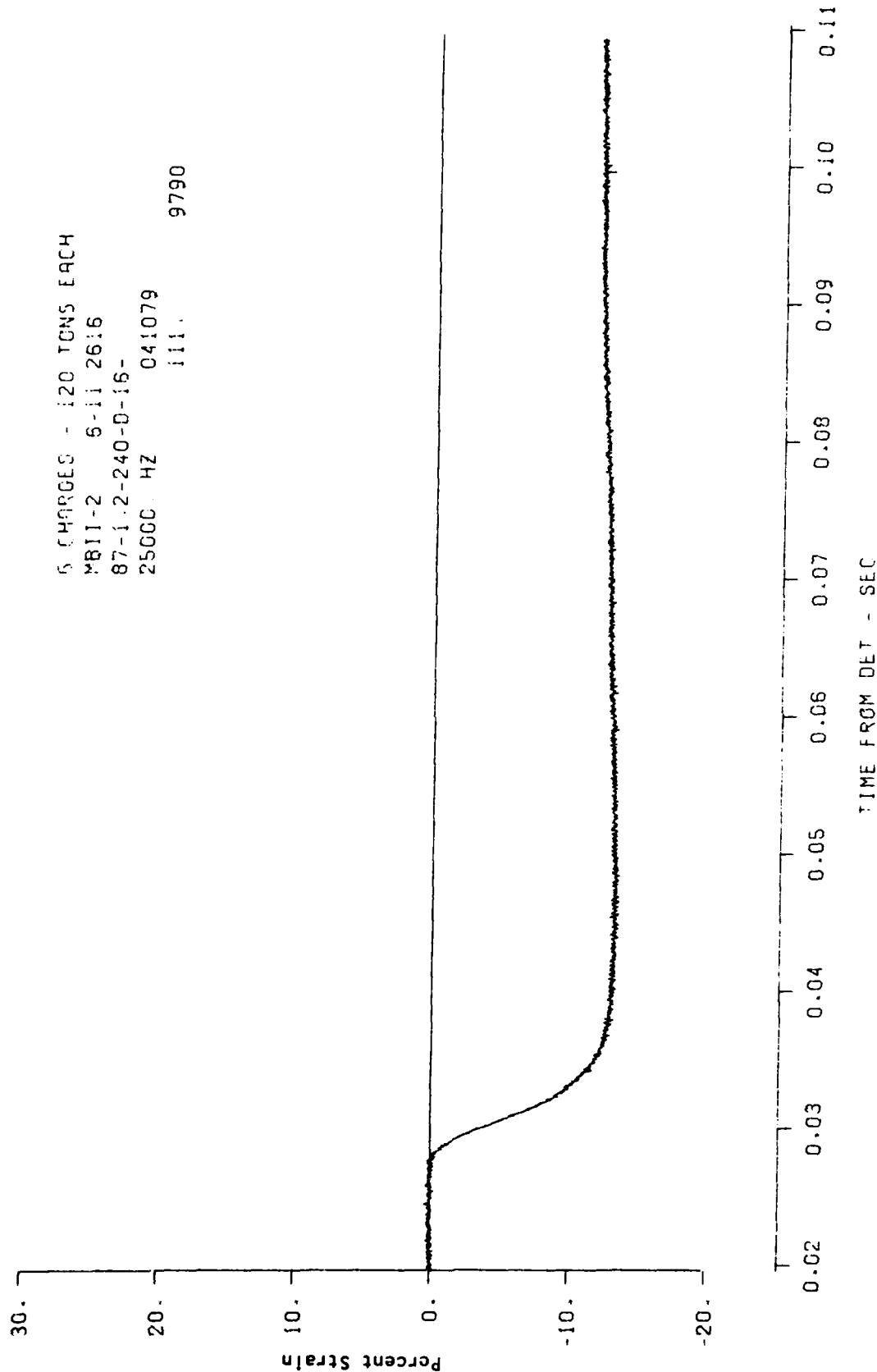


Figure 11. Vertical strain at 87 m, 1.2 m depth and 240° azimuth.



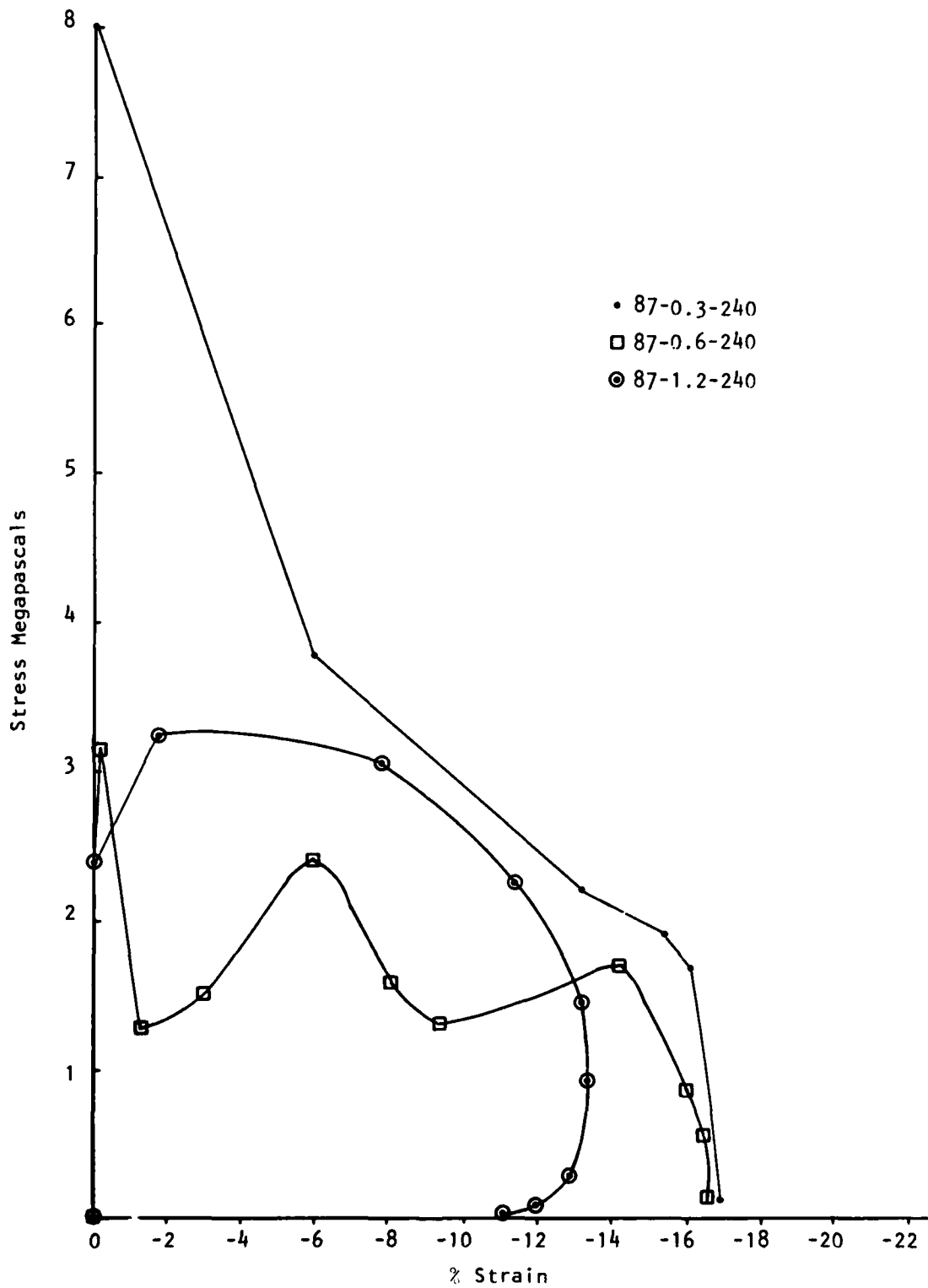


Figure 12. Dynamic stress-strain curves for three depths at 87 m, 240° azimuth.

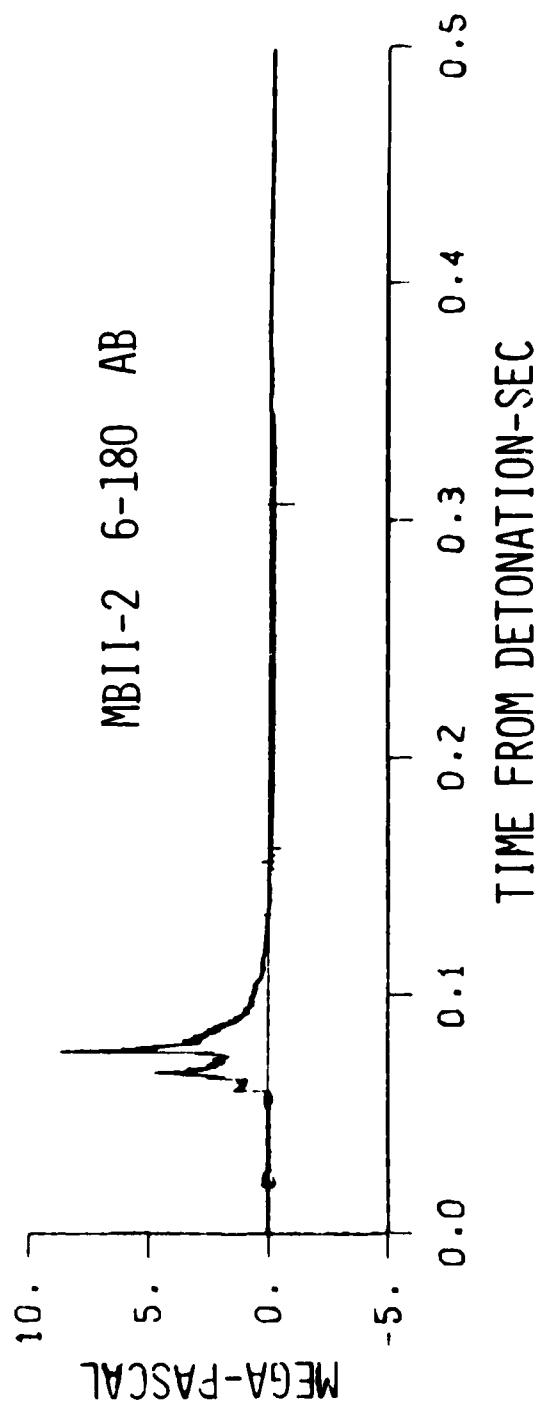


Figure 13. Air blast wave form at 180° and 6 m from center of the array over strain gage emplacement.

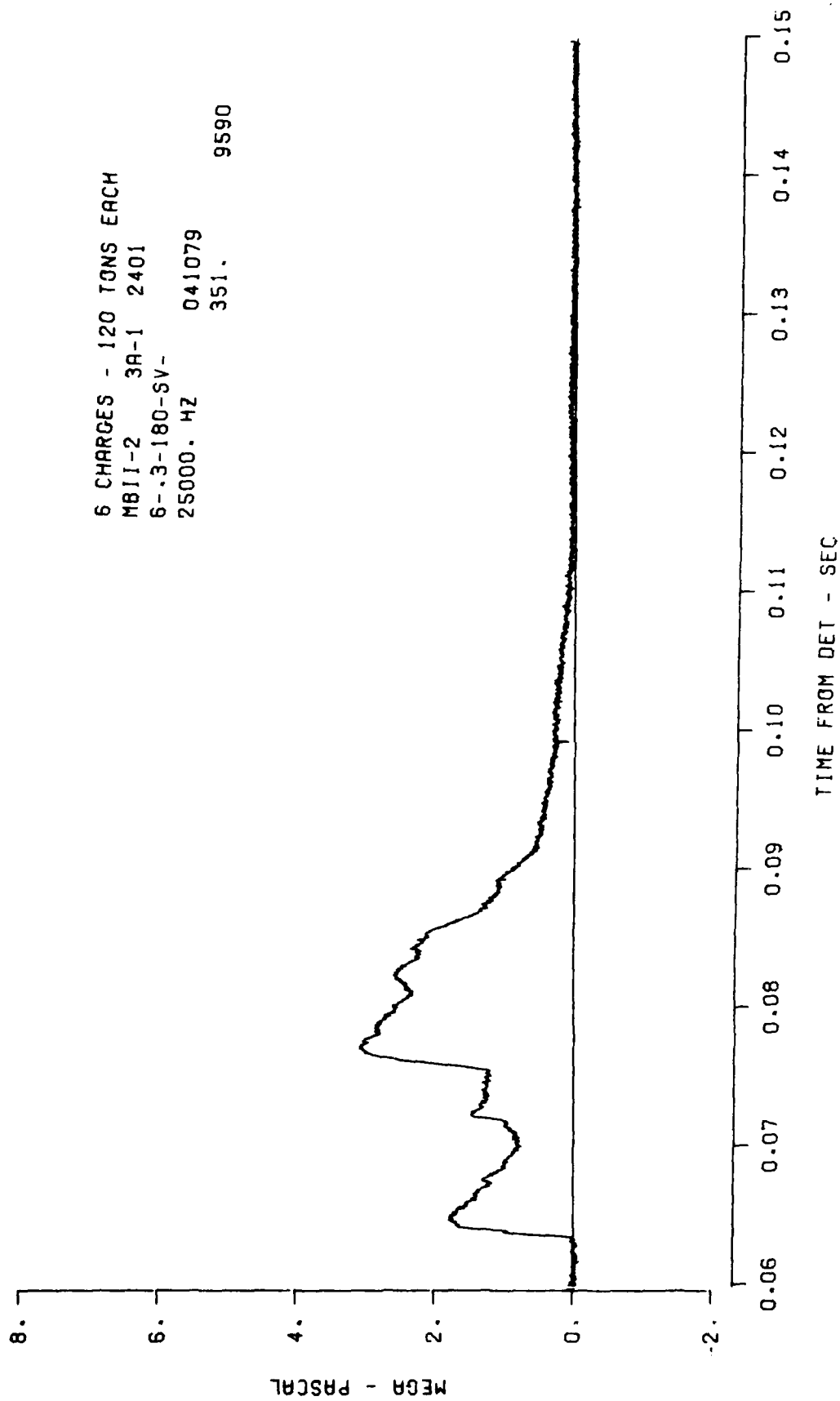


Figure 14. Vertical stress at 6 m, 0.3 m depth and 180° azimuth.

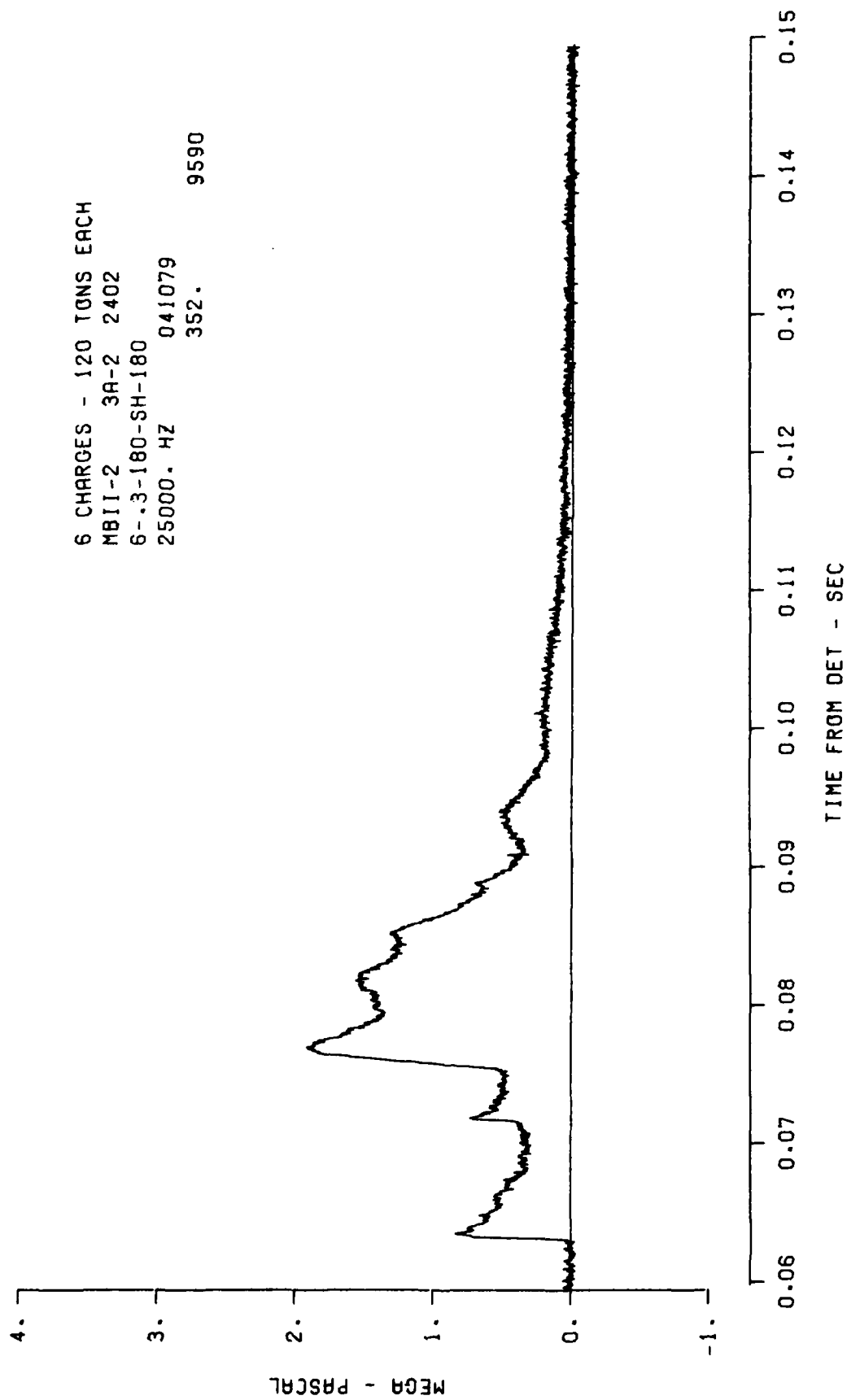


Figure 15. Horizontal stress at 6 m, 0.3 m depth and 180° azimuth.

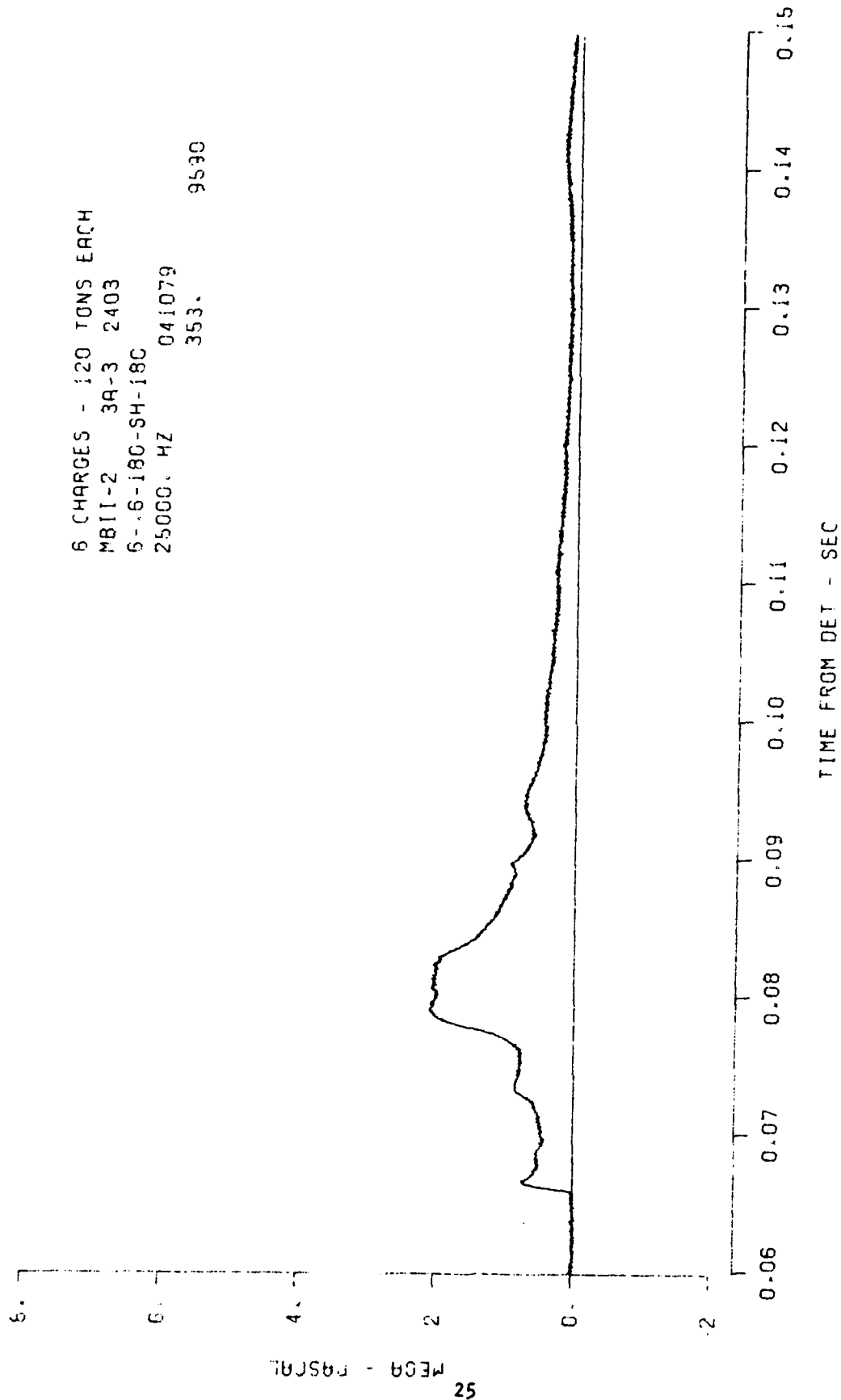


Figure 16. Horizontal stress at 6 m, 0.6 m depth and 180° azimuth.

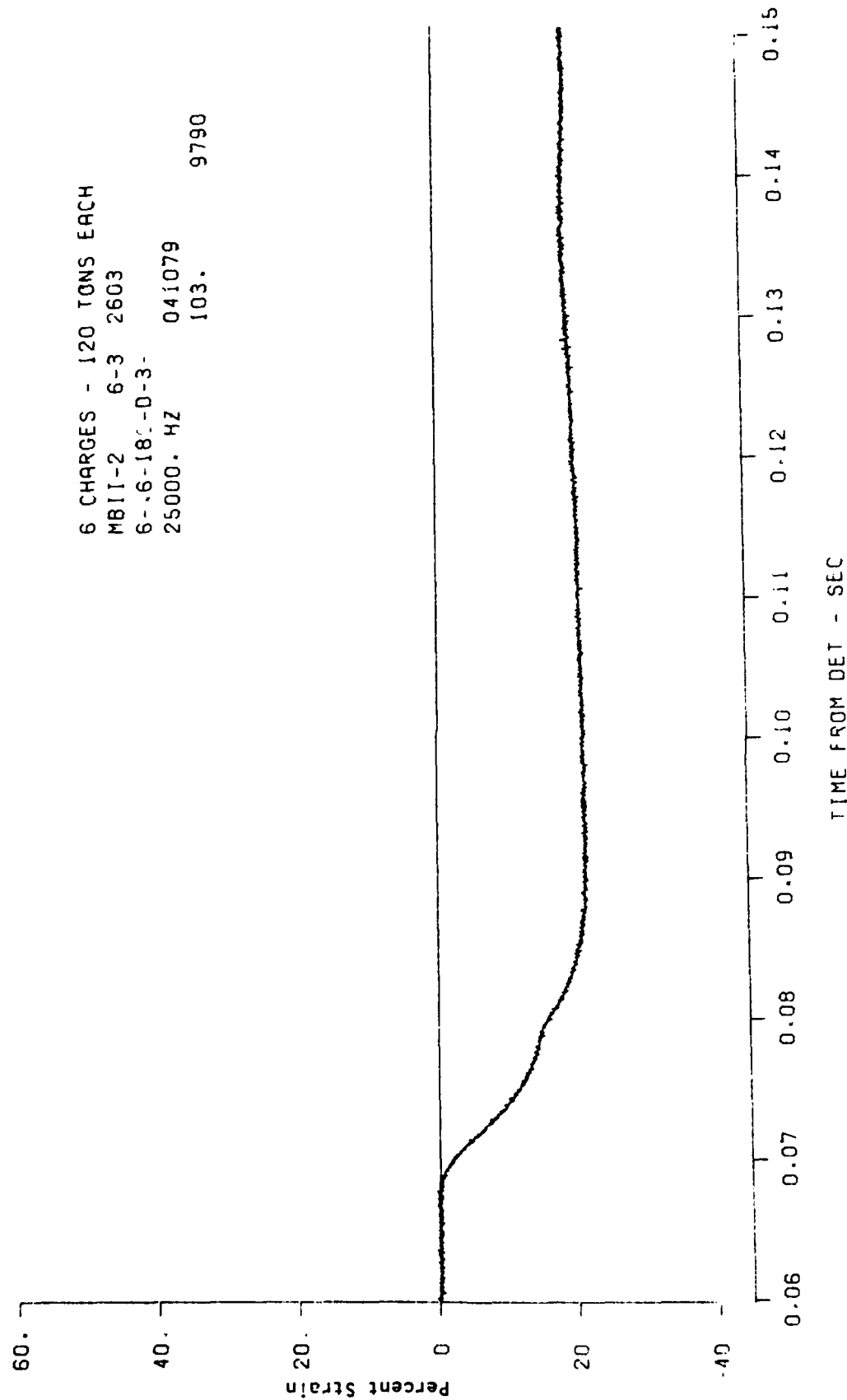


Figure 17. Vertical strain from 6 m, 0.6 m depth and 180° azimuth.

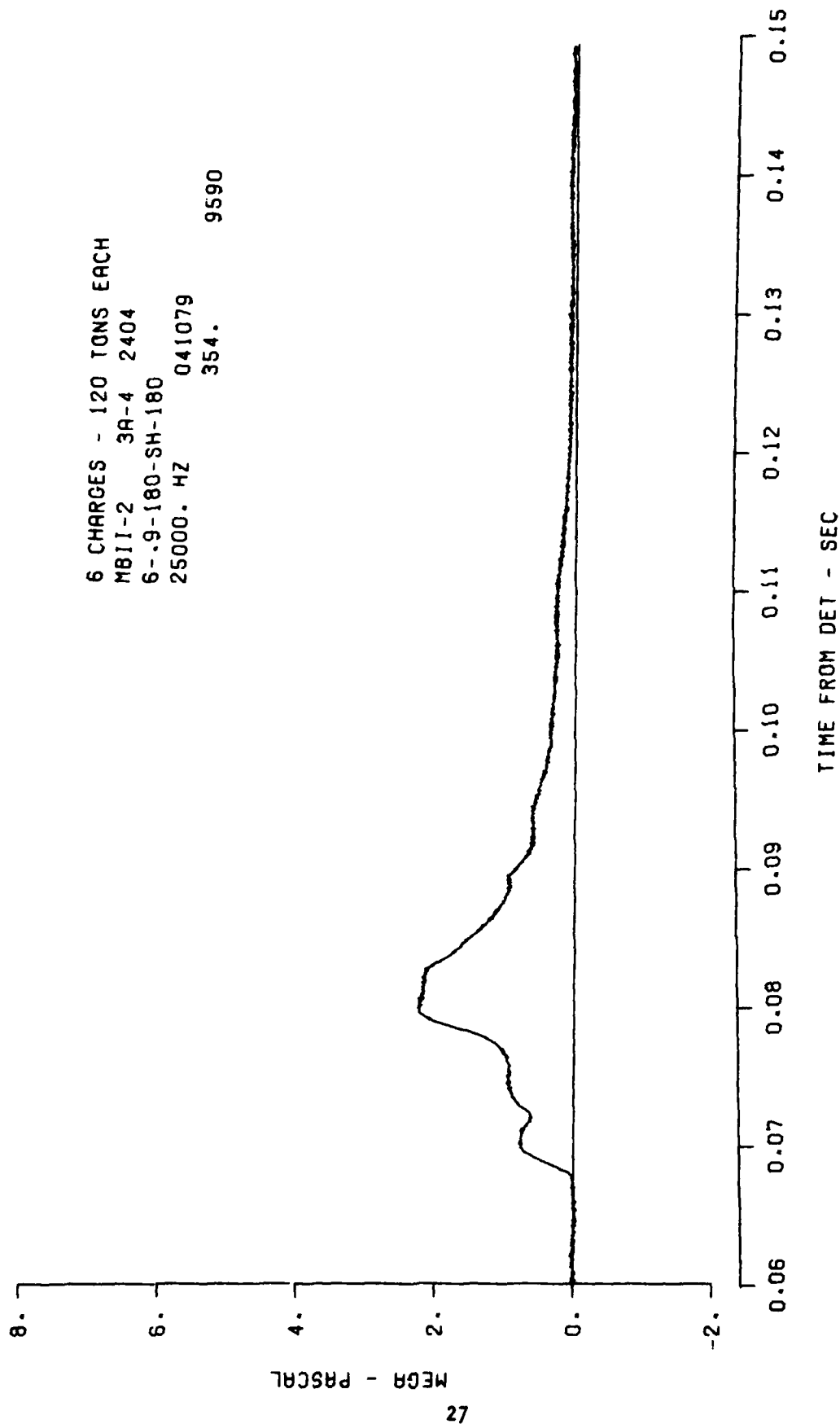


Figure 18. Horizontal stress from 6 m, 0.9 m depth and 180° azimuth.

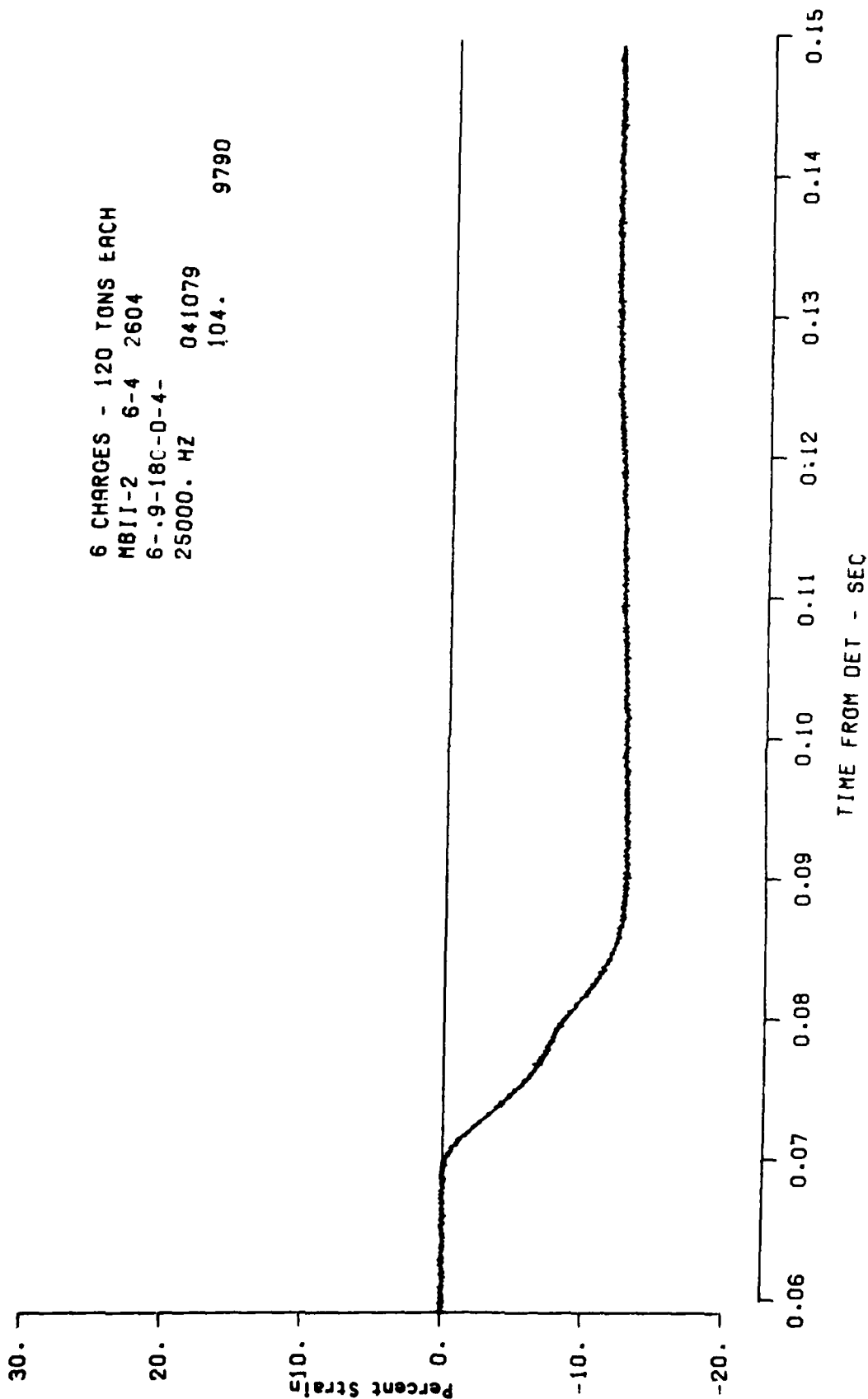


Figure 19. Vertical strain from 6 m, 0.9 m depth and 180° azimuth.



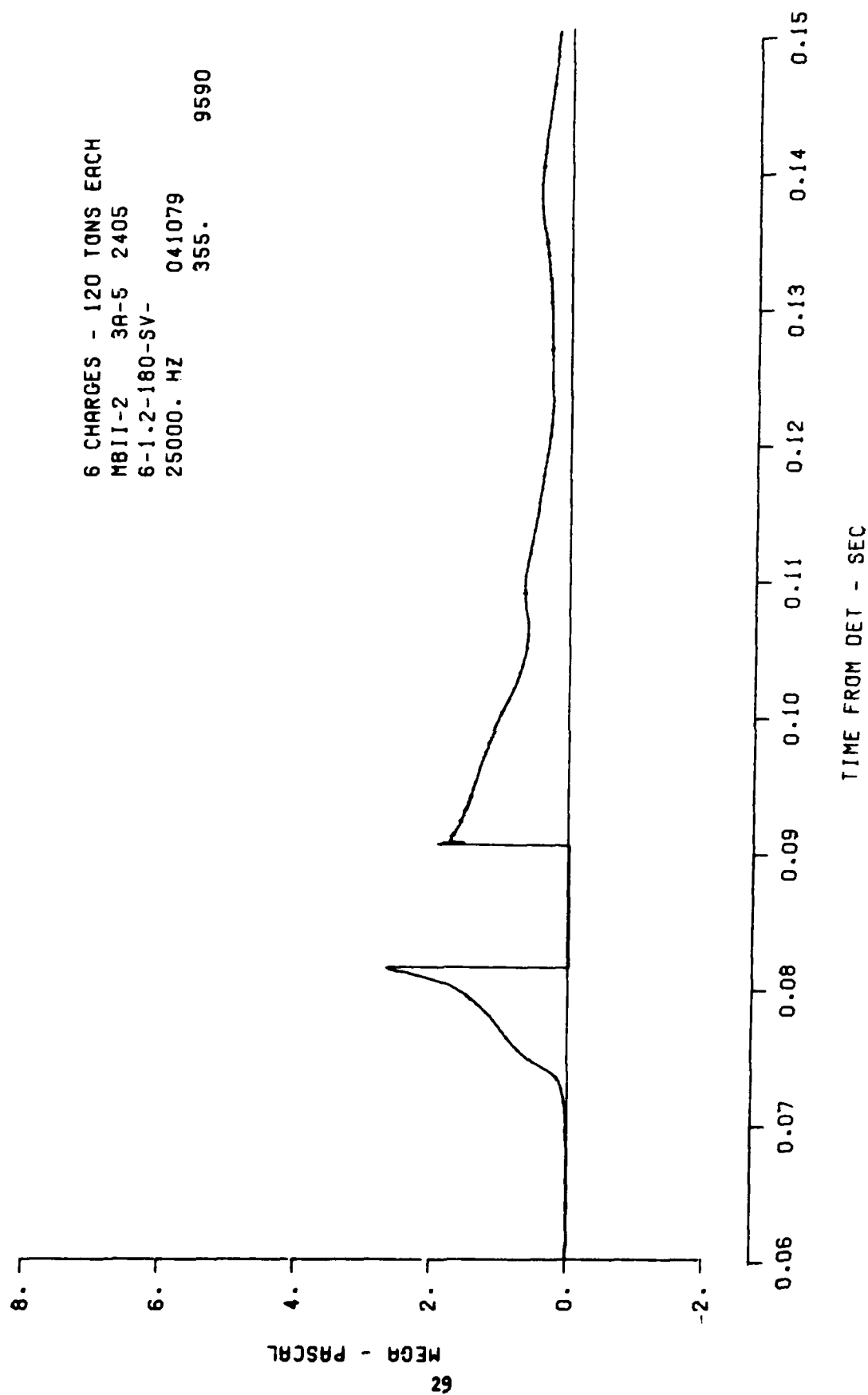


Figure 20. Vertical stress from 6 m, 1.2 m depth and 180° azimuth.

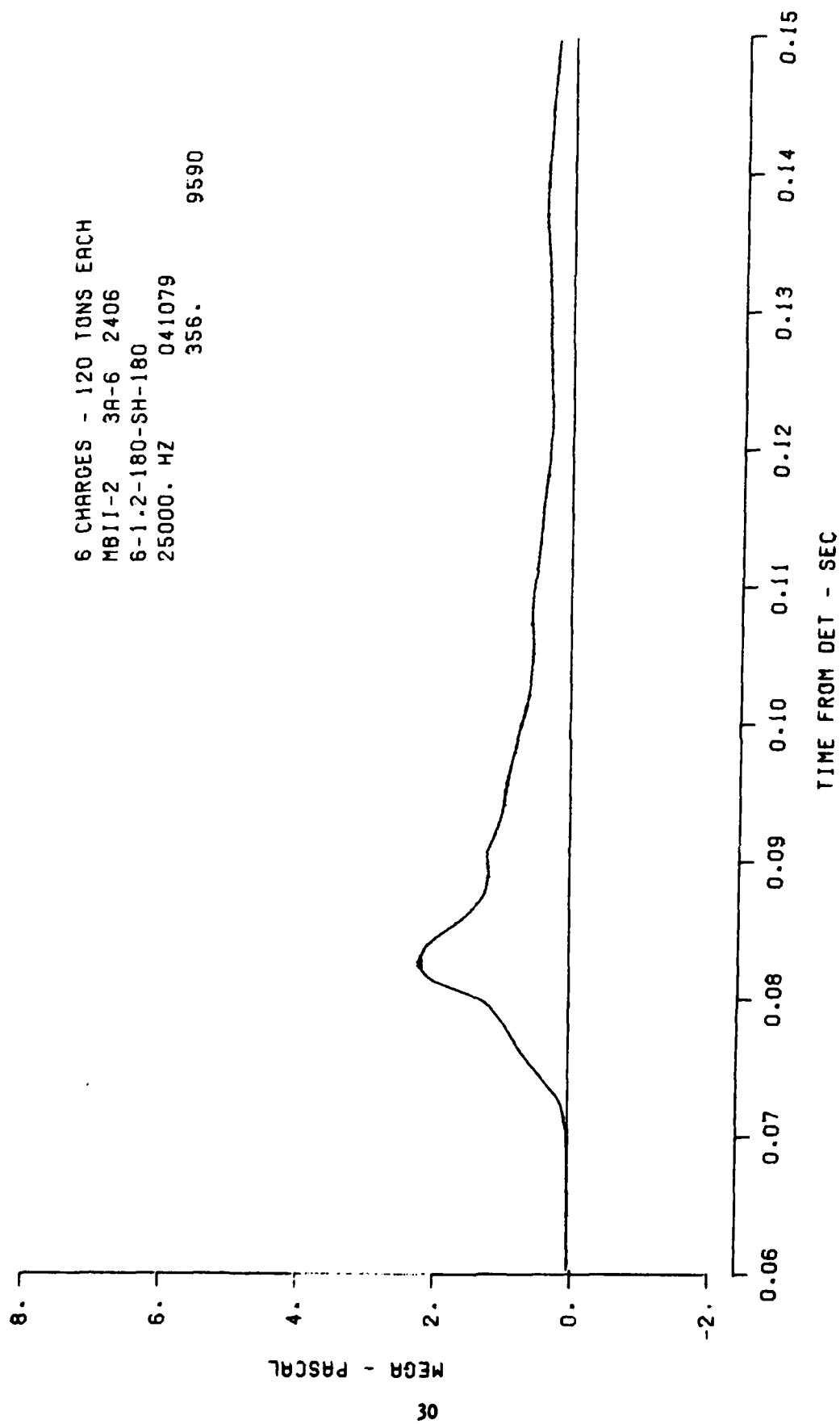


Figure 21. Horizontal stress at 6 m, 1.2 m depth and 180° azimuth.

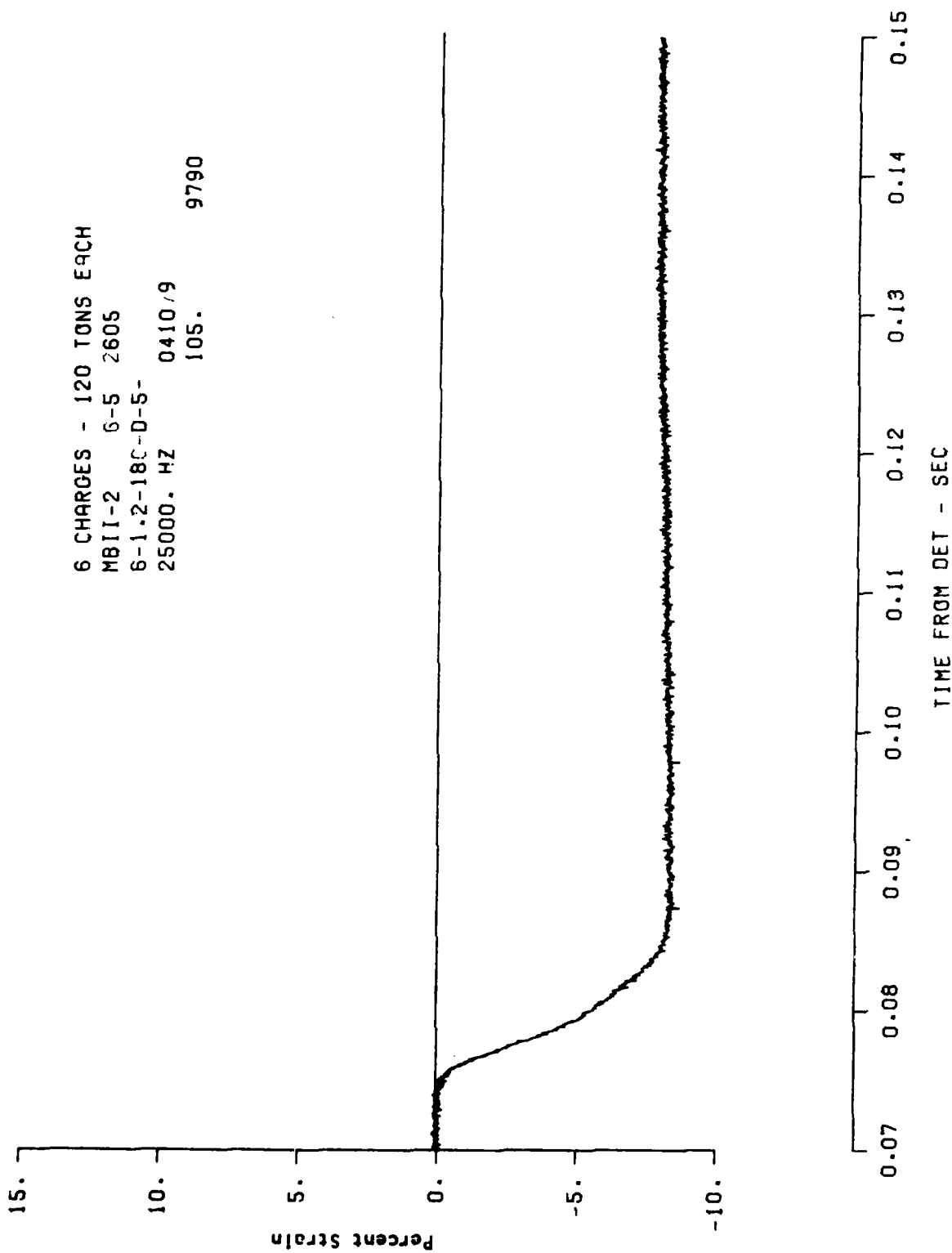


Figure 22. Vertical strain at 6 m, 1.2 m depth and 180° azimuth.

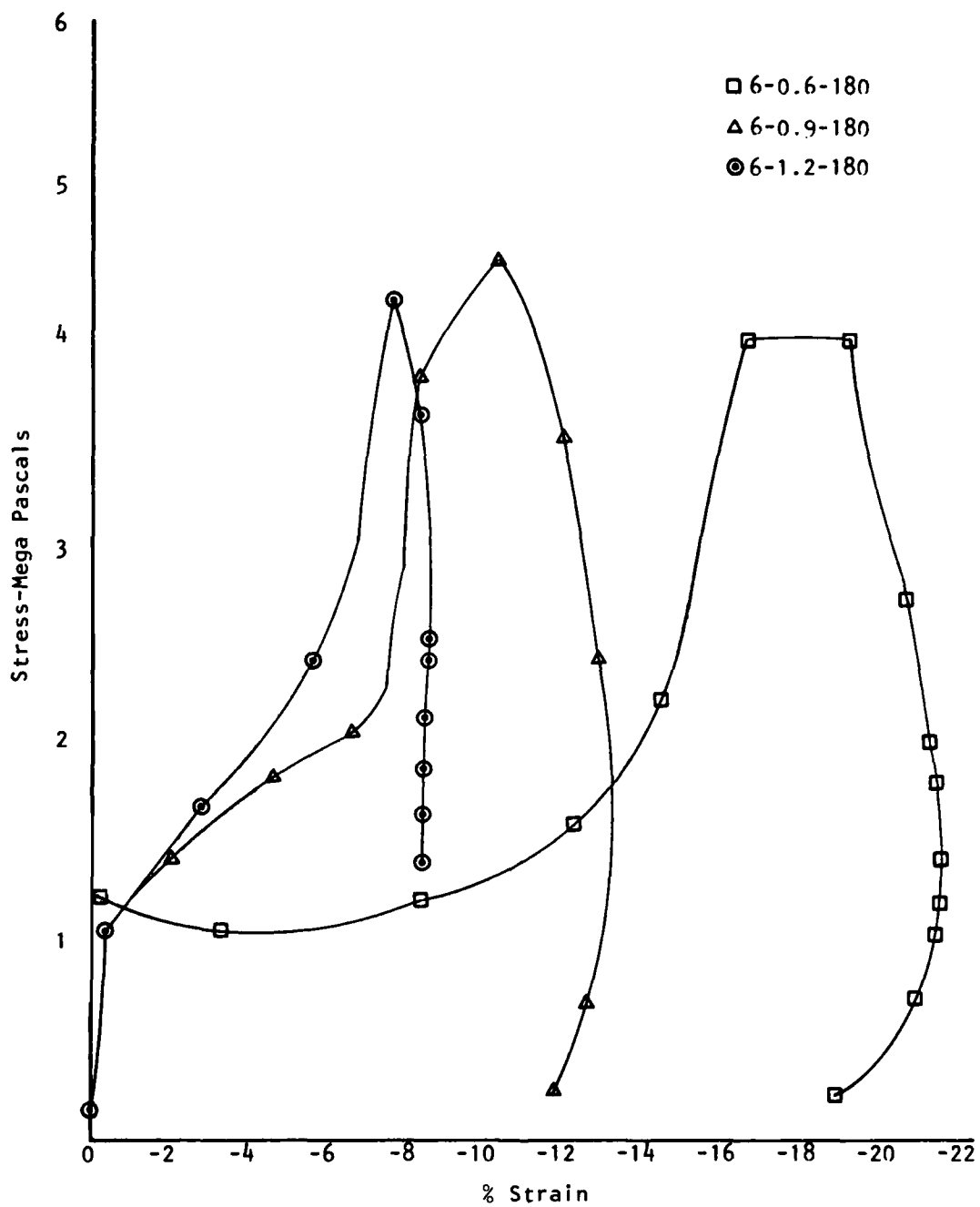


Figure 23. Dynamic stress-strain curves for three depths at 6 m, 180° azimuth.

## DISTRIBUTION LIST

### DEPARTMENT OF DEFENSE

Assistant to the Secretary of Defense  
Atomic Energy

ATTN: Executive Assistant

Defense Technical Information Center  
12 cy ATTN: DD

Defense Nuclear Agency

ATTN: DDST

ATTN: SPTD

4 cy ATTN: TITL

2 cy ATTN: SPSS

Field Command

Defense Nuclear Agency

ATTN: FCT

ATTN: FCTMOF

ATTN: FCPR

Field Command

Defense Nuclear Agency

ATTN: FCPR

Undersecretary of Def. for Rsch. & Engrg.  
ATTN: Strategic & Space Systems (OS)

### DEPARTMENT OF THE ARMY

Harry Diamond Laboratories

Department of the Army

ATTN: DELHD-N-P

ATTN: DELHD-I-TL

U.S. Army Ballistic Research Labs.

ATTN: DRDAR-BLT, W. Taylor

ATTN: DRDAR-TSB-S

ATTN: DRDAR-BLE, J. Keefer

ATTN: DRDAR-BLV

U.S. Army Cold Region Res. Engr. Lab.

ATTN: CRREL-EM

U.S. Army Engr. Waterways Exper. Station

ATTN: L. Ingram

ATTN: G. Jackson

ATTN: J. Strange

ATTN: J. Ingram

ATTN: W. Flathau

ATTN: F. Hanes

ATTN: Library

U.S. Army Nuclear & Chemical Agency

ATTN: Library

### DEPARTMENT OF THE NAVY

Naval Surface Weapons Center

ATTN: Code F31

### DEPARTMENT OF THE AIR FORCE

Space & Missile Systems Organization

Air Force Systems Command

ATTN: DEB

### DEPARTMENT OF THE AIR FORCE (Continued)

Air Force Weapons Laboratory

Air Force Systems Command

ATTN: DED, R. Matalucci

ATTN: DE, M. Plamondon

ATTN: DEX, J. Renick

ATTN: DES-C, R. Henny

ATTN: SUL

ATTN: DEX

Space & Missile Systems Organization

Air Force Systems Command

ATTN: MMH

ATTN: MNNH

### DEPARTMENT OF DEFENSE CONTRACTORS

Acurex Corp.

ATTN: K. Triebes

Aerospace Corp.

ATTN: P. Mathur

ATTN: Technical Information Services

Agbabian Associates

ATTN: M. Agbabian

Analytic Services, Inc.

ATTN: G. Hesselbacher

Applied Theory, Inc.

2 cy ATTN: J. Trulio

Artec Associates, Inc.

ATTN: D. Baum

ATTN: S. Gill

AVCO Research & Systems Group

ATTN: Library A830

BDM Corp.

ATTN: T. Neighbors

ATTN: A. Lavagnino

ATTN: Corporate Library

BDM Corp.

ATTN: R. Hensley

Boeing Co.

ATTN: B. Lempriere

ATTN: Aerospace Library

ATTN: R. Carlson

California Research & Technology, Inc.

ATTN: K. Kreyenhagen

ATTN: Library

Civil Systems, Inc.

ATTN: J. Bratton

DEVELCO, Inc.

ATTN: L. Rorden

EG&G Washington Analytical Services Center, Inc.

ATTN: Library

DEPARTMENT OF DEFENSE CONTRACTORS (Continued)

Electromechanical Sys. of New Mexico, Inc.  
ATTN: R. Shunk

Eric H. Wang  
Civil Engineering Rsch. Fac.  
ATTN: N. Baum

General Electric Company-TEMPO  
ATTN: DASIAC  
ATTN: J. Shoutens

H-Tech Labs, Inc.  
ATTN: B. Hartenbaum

Merritt CASES, Inc.  
ATTN: J. Merritt  
ATTN: Library

Physics International Co.  
ATTN: Technical Library  
ATTN: L. Behrmann  
ATTN: E. Moore  
ATTN: F. Sauer

R & D Associates  
ATTN: R. Port  
ATTN: Technical Information Center  
ATTN: J. Carpenter  
ATTN: W. Wright, Jr.  
ATTN: J. Lewis  
ATTN: A. Kuhl  
10 cy ATTN: A. Latter  
ATTN: C. MacDonald

R & D Associates  
ATTN: H. Cooper

DEPARTMENT OF DEFENSE CONTRACTORS (Continued)

Science Applications, Inc.  
ATTN: Technical Library

Science Applications, Inc.  
ATTN: K. Sites

SRI International  
ATTN: B. Gasten/P. De Carli  
ATTN: G. Abrahamson

Systems, Science & Software, Inc.  
ATTN: T. Cherry  
ATTN: Library  
ATTN: D. Grine  
ATTN: T. Riney

Tetra Tech, Inc.  
ATTN: L. Hwang  
ATTN: Library

TRW Defense & Space Sys. Group  
ATTN: P. Bhutta  
ATTN: Technical Information Center  
ATTN: D. Baer  
ATTN: R. Plebuch  
2 cy ATTN: P. Dai  
ATTN: I. Alber

TRW Defense & Space Sys. Group  
ATTN: E. Wong

Weidlinger Assoc., Consulting Engineers  
ATTN: M. Baron